Soft Matter

DOI: 10.1002/ange.201301128

A Gel-Based Trihybrid System Containing Nanofibers, Nanosheets, and Nanoparticles: Modulation of the Rheological Property and Catalysis**

*Jayanta Nanda, Abhijit Biswas, Bimalendu Adhikari, and Arindam Banerjee**

Materials based on low-molecular-weight gels[1] (LMWGs) are an emerging field of research because of their applications in different fields including photovoltaic cells,[2a] organic light-emitting diodes,[2b] sensing,[2c] oil spill recovery,[2d] removal of toxic dyes,[2e–f] and delivery of drugs and biomolecules[2g] and others.[2h] These supramolecular gels generally form a nanofibrillar network structure, in which a variety of nanomaterials can be encapsulated to form hybrid systems.[3,4] Recently, the formation of hybrid-gel-based functional soft materials has attracted significant interest by incorporating different metal/semiconducting inorganic nanomaterials[3] as well as carbon-based nanomaterials[4] into the gel matrix. Most of these hybrid materials are endowed with interesting properties and applications, such as the modulation of conductivity, sensing, and improved mechanical strength among others.[3,4] However, recent advancement in nanomaterials research includes graphene/graphene-oxide-based nanomaterials because of their exceptional physical, chemical, and materials properties.[5] Construction and analysis of graphene- and graphene-oxide-based nanomaterials have gained significant attention now a days.[6] Zhang and co-workers have made a significant contribution regarding graphene-based hybrid nanomaterials.[5c,6g] Graphene oxide is a fascinating building block to construct different supramolecular entities including gels.[7] There are a few examples of graphene-oxide-based gels.[7] Shi and co-workers have recently developed graphene oxide/DNA composite hydrogels, graphene oxide/hemoglobin composite hydrogels, and graphene oxide/poly(vinyl alcohol) composite hydrogels.[7a–d] Creation of gel-based homogeneous functional hybrid system is needed in current advanced nanomaterials research. There is a real need for making graphene/graphene oxide and metal-nanoparticle-containing functional hybrid system that can exhibit incremental improvement of physical, chemical, mechanical, and material properties of hybrid-gel materials by stepwise incorporation of different nanomaterials into the native gel matrix.

A pyrene-appended aromatic amino-acid- (tryptophan-) based supramolecular hydrogel has been discovered in phosphate buffer solution. This hydrogel material can be exploited to make a trihybrid system by stepwise inclusion of graphene oxide (GO)/graphene and metal nanoparticles. Our gelator molecule has the unique property to interact with the π-molecular surface of graphene oxide (GO) sheets using π–π interactions[8] as it has an aromatic side-chain residue (Trp) and an N-terminally blocked pyrene residue. Moreover, this gelator has a redox-active moiety (Trp) and it has been used for the reduction of gold salt (Au^{3+}) to gold nanoparticles (AuNPs) at room temperature within the GO-containing hybrid hydrogel matrix to prepare a more complex trihybrid hydrogel. A trihybrid hydrogel has been prepared by stepwise incorporation of graphene oxide first and then, synthesizing gold nanoparticles in situ within the GO-containing hydrogel matrix. The choice for making a native gelator molecule is perfect so that not only graphene/graphene oxide can be incorporated into the system but also a gold salt (Au^{3+}) can be in situ reduced to gold nanoparticles within the gel matrix to form a novel trihybrid system.

The morphology of the trihybrid hydrogel reveals the coexistence of three distinctly different nanostructures including amino-acid-based nanofibers, graphene oxide (GO) nanosheets, and gold nanoparticles. Rheological studies of the native gel and the hybrid gels reveal a stepwise increase of the storage modulus (G') and the yield stress (σ_y) by a stepwise incorporation of graphene oxide and gold nanoparticles into the native hydrogel matrix. The catalytic activity (reduction of nitroarene to aminoarene) of the gold nanoparticles in the native gel matrix is also increased in the presence of graphene oxide in the trihybrid system.

A pyrene-conjugated tryptophan-based (Py-W) supramolecular hydrogelator (Figure 1a) has been developed in phosphate buffer solution at pH 7.3 to 8.7. Gelation of Py-W was induced by sonication (Figure 1b,c). The minimum gelation concentration (MGC) of the gelator has been found to be 0.83% (w/v). The morphology of the hydrogel has been studied by using various microscopic techniques including fluorescence microscopy (Figure S7), field emission scanning electron microscopy (FE-SEM), and transmission electron microscopy (TEM). Figure 1d and e shows the FE-SEM and TEM images of the hydrogel indicating a nanofibrillar network structure upon self-association. Widths of these gel nanofibers obtained from the FE-SEM and TEM studies (Figure 1d and e) are in the range of 35–60 and 40–

[*] Dr. J. Nanda, A. Biswas, Dr. B. Adhikari, Prof. A. Banerjee
Department of Biological Chemistry
Indian Association for the Cultivation of Science
Jadavpur, Kolkata 700 032 (India)
E-mail: bcab@iacs.res.in

[**] Abhijit thanks the CSIR, New Delhi, India, for financial assistance. We also thank DST, Government of India for financial support (project number SR/S1/OC-73/2009). The authors thank for support of the XPS facility from the DST Unit of Nanoscience at the Indian Association for the Cultivation of Science.

Supporting information for this article is available on the WWW under http://dx.doi.org/10.1002/anie.201301128.

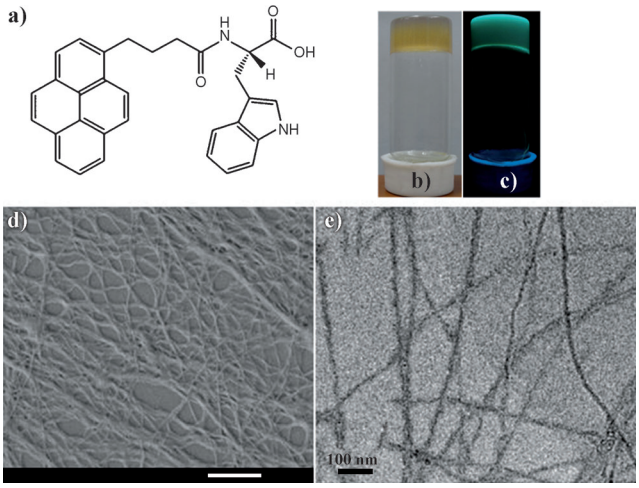

Figure 1. a) Chemical structure of the gelator (Py-W), inverted gel vial b) under daylight and c) under UV light. d) SEM (scale bare = 1 μm) and e) TEM images of the hydrogel.

55 nm, respectively. Fourier-transformed infrared spectra (FT-IR) have been used to characterize the structure of the gelator (Py-W) within the hydrogel matrix at molecular scale. A FT-IR study of the gelators in the xerogel state has been performed (Figure S8). A peak at 1633 cm^{-1} has been observed for the amide carbonyl stretching frequency. It is a characteristic signature of a β-sheet-like conformation.[3e]

In this study, graphene oxide (GO) has been incorporated into the native hydrogel matrix. GO has a two-dimensional carbon nanostructure (sheet) with plenty of hydrophilic oxygenated groups (hydroxyl, epoxide, and carboxylic group). At first, the hydrogel (Py-W) has been prepared and then graphene oxide has been incorporated into this hydrogel matrix to prepare a dihybrid gel (Py-W/GO) system (Figure S9). Interestingly, sonication is not required to make a GO-containing hybrid hydrogel preparation. The presence of GO in the hybrid hydrogel has lowered the gelation concentration of the native hydrogel.

The gelator molecule has one Trp residue which has been used to incorporate gold nanoparticles in the GO-containing hybrid hydrogel matrix by a heating–cooling cycle using an auric chloride solution. This gives rise to another self-supported reddish colored hydrogel (Figure S9). It is known in literature that Trp is an excellent redox-active amino acid residue which can reduce silver/gold ions into their metallic state.[9] The color change is due to the reduction of the gold salt into the corresponding metallic nanoparticles. The nascently formed AuNPs have been stabilized within the network structure of the hydrogel matrix and this prevents the aggregation of gold nanoparticles. Formation of the gold nanoparticles has been supported by the X-ray diffraction (XRD) study of a trihybrid gel. The XRD pattern for the trihybrid gel has shown diffraction peaks at $2\theta = 38.2$ and 44.3°. All these XRD peaks are corresponding to in situ synthesized AuNPs within the gel matrix (Figure S10). These diffraction peaks correspond to (111) and (200) Miller indices of metallic Au, respectively. Moreover, the presence of AuNPs has also been confirmed by XPS analysis (Figure S11). The Trp residue can only reduce the Au^{3+} ions to metallic nanoparticles and is unable to reduce GO to form reduced graphene oxide (RGO).[7f] This observation is also well-supported by Raman spectral analysis (Figure S12). Two fundamental vibrations are present in both of these materials at 1350 and 1588 cm^{-1} corresponding to the D and G band of GO, respectively. The G band corresponds to the first-order scattering of the E_{2g} mode of sp^2 C atoms and the D band corresponds to the A_{1g} symmetry mode. The intensity ratios of the D and G bands are almost similar in two hybrid gels and this implies that GO is not reduced within the hydrogel matrix.

The morphology of the hybrid hydrogel has been studied by using FE-SEM and TEM after formation of a hybrid hydrogel with more than one type of nanomaterial. FE-SEM and TEM images of GO containing hybrid hydrogel are shown in Figure 2a and Figures S13 and S14b. In these electronic microscopic studies, two distinct morphologies have been simultaneously observed: a) gel nanofibers (coming from the amino-acid-based native hydrogel) and b) the flat morphology of graphene oxide nanosheets.

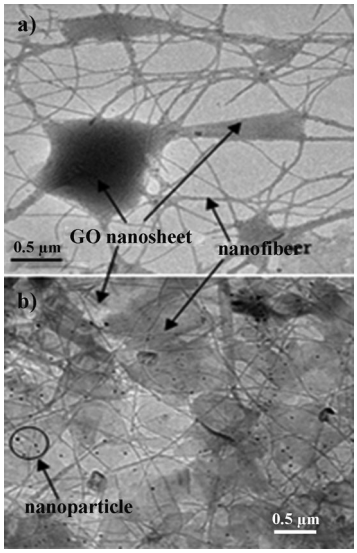

Figure 2. TEM images of a) a dihybrid gel showing the presence of both the nanofibers and nanosheets and b) a trihybrid gel with three distinct morphologies: nanoparticles, nanosheets, and nanofibers as indicated in the picture.

This indicates that the morphology of the amino-acid-based fibrillar network structure is maintained here and it is a true hybrid system. Incorporation of graphene oxide in the hydrogel matrix does not affect fibril formation. Sometimes, these nanofibers are on the surface of a GO sheet (Figure 2a). This is probably due to the aromatic interaction of the gelator molecules and the large planner aromatic surface of the graphene oxide sheets.[4b] Moreover, in the trihybrid system, three distinctly different morphologies have been observed with a combination of nanofibers, nanosheets, and nanoparticles (Figure 2b).

Figure S15a shows the magnified image of in situ synthesized gold nanoparticles. The size distribution profile diagram of gold nanoparticles has also been obtained from the TEM image of gold nanoparticles (Figure S15b). The presence of gold nanoparticles has been confirmed by energy-dispersive X-ray (EDX) analysis (Figure S15c). Preparation of a trihybrid from such a unique system containing three types of nanomaterials including amino-acid-based nanofibers, carbon-based graphene oxide sheets, and gold nanoparticles has a promising future in materials science. To the best of our knowledge, this is the first report of coexistence of three such nanomaterials (nanofibers, nanosheets, and nanoparticles) in a hybrid system.

Rheological studies of native hydrogel and hybrid hydrogels have been performed to address whether rheological properties of hybrid hydrogels are different from that of the native gel. Oscillatory stress sweep experiments have been performed at 25 °C. From Figure 3, it has been observed that

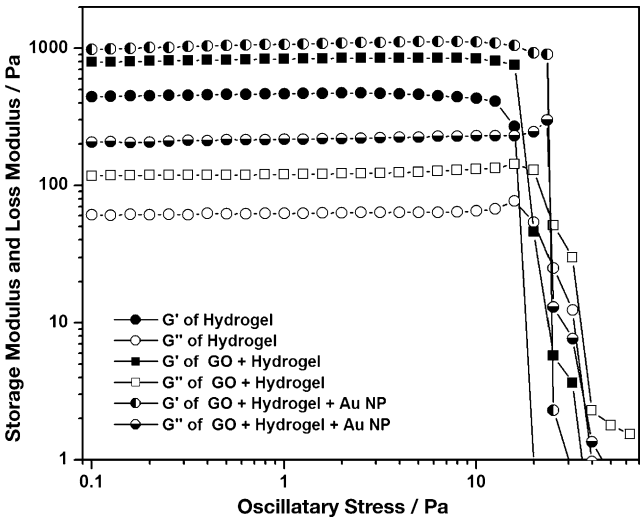

Figure 3. Oscillatory stress sweep experiments for a native hydrogel, GO-based hydrogel, and trihybrid hydrogel as indicated in the picture suggesting the breakage of these gels under a particular stress.

in the linear viscoelastic region (LVR), the storage modulus (G′) is higher than the loss modulus (G″). This is an indication of the formation of a typical soft solid-like gel-phase material.[4a,10] Similarly, oscillatory stress sweep experiments have also been performed on the hybrid hydrogels. For hydrogel and hybrid hydrogels, the initially storage modulus (G′) is higher than the loss modulus (G″) suggesting the formation of the gel-phase material. After the LVR region, the loss modulus (G″) has crossed the storage modulus and has transformed into solution state. This particular stress value is called yield stress (σ_y). Storage modulus values at oscillatory stress 0.126 Pa and yield stress values are summarized in the Table S1. From Table S1, it is evident that the storage modulus (G′) and the yield stress (σ_y) values gradually increase when graphene oxide and gold nanoparticles are stepwise incorporated into the native gel. It is also evident from Table S1 that the storage modulus (G′) and the yield stress (σ) values follow the order: trihybrid gel (Py-W/GO/AuNPs) > dihybrid gel (Py-W/GO) > native gel (Py-W). There are several examples for the increment of the stiffness of the hybrid gel upon incorporation of carbon-based nanomaterials or metal nanoparticles into the native gel.[4,10d–e] However, our result is a unique example of a stepwise increment of the mechanical strength of the gel in a trihybrid system indicating the tailor-made modulation of rheological properties of the gel-phase material in a hybrid system.

The mechanical strength of the dihybrid hydrogel probably increases because of the π–π stacking and hydrogen-bonding interactions between the gelator molecules and GO sheets in the hybrid gel system. Each gelator molecule contains a large aromatic pyrene group and an aromatic indole residue (Trp) and they support the interactions between the gelator molecules and GO sheets containing a large π surface. Interaction of the pyrene group with GO has been evidenced by fluorescence spectroscopy. The pyrene-conjugated amino-acid-based hydrogel shows a broad emission peak centered at 498 nm and this peak is due to the formation of the pyrene excimer in the gel state (Figure S16). However, the fluorescence intensity of the hydrogels has been quenched significantly in the presence of GO in both the dihybrid and trihybrid gels (Figure S16);[4a,6g] this quenching might be due to the presence of sufficient π–π interactions between aromatic groups of the gelator and GO in the dihybrid and trihybrid systems.[11]

The Trp residue within the gelator molecule has been nicely used for in situ synthesis and stabilization of gold nanoparticles within the GO-containing hybrid hydrogel matrix. As a consequence the nascently formed AuNPs are bringing the gelator (Py-W) molecules closer to one another and this actually favors the interactions between the gel nanofiber strands. Most probably, this results in an increase in the mechanical strength of the trihybrid system more than that of the dihybrid gel (Py-W/GO) system. This observation is supported by a recent result, where in situ reduction of AuNPs within the hydrogel matrices has enhanced the mechanical stiffness of the hybrid hydrogels.[10e] There are also several reports about an increase in the stiffness of the hybrid gel upon incorporation of metal nanoparticles from the outside into the native gel matrix.[7e,10e] This study has vividly demonstrated the stepwise increment of gel stiffness upon incorporation of first carbon nanomaterials (GO) and then, metal nanoparticles (AuNPs) into the hydrogel system. The stiffness of the hydrogel can be manipulated by the incremental incorporation of carbon-based nanomaterials and gold nanoparticles into the hydrogel system. Modulation of the rheological behavior has been remarkably noticed in this report as the storage modulus and yield stress of the hybrid gel can be gradually increased by incorporation of graphene oxide and gold nanoparticles. This example of gradual increase of mechanical strength in the gel phase of a hybrid gel system relative to that of a native gel may lead to new advanced materials with interesting properties.

Graphene-supported metal-nanoparticle-embedded materials have become highly important in catalysis because of their large surface area, high electronic transport capacity, and extraordinary mechanical strength.[7g,12] To probe the

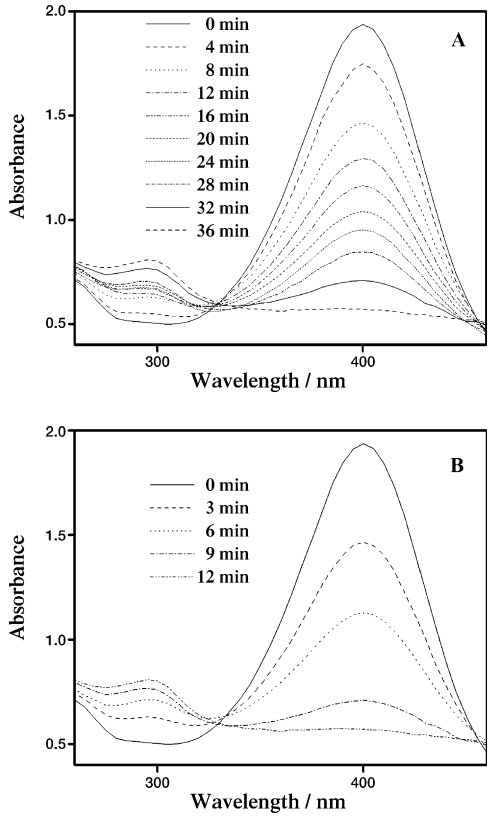

Figure 4. UV/Vis spectra of the catalytic reduction of 4-nitrophenol in the presence of different catalysts: A) dihybrid-1 (Py-W/AuNPs) and B) trihybrid (Py-W/GO/AuNPs).

catalytic activity of our newly synthesized trihybrid system (Py-W/GO/AuNPs), the functional group transformation of 4-nitrophenol in the presence of sodium borohydride ($NaBH_4$) has been chosen as an exemplary reaction (Figure 4). For this purpose, the trihybrid hydrogel has been freeze-dried in a lyophilizer. The 4-nitrophenol shows an absorbance peak at about 317 nm and it has been red-shifted to 400 nm in the presence of $NaBH_4$ because of the formation of the 4-nitrophenolate ion in alkali medium. However, no transformation (reduction) has been observed under this condition in the absence of any catalyst. In the presence of trihybrid material (xerogel), the depletion of the 4-nitrophenol peak at 400 nm and the concomitant increase of a peak at 297 nm has been monitored over time (Figure 4B). This is indicative of the formation of 4-aminophenol. Another catalytic system dihybrid-1 (Py-W/AuNPs) has been prepared by synthesizing AuNPs within the Py-W hydrogel to compare the catalytic activity with the trihybrid system having the same amount of gold nanoparticles in different environments. The rate of the catalytic reaction of dihybrid-1 is $3.021 \times 10^{-2}\ min^{-1}$, whereas that of the trihybrid system is $10.578 \times 10^{-2}\ min^{-1}$ (Figure S18). This indicates the better efficiency of the trihybrid catalyst compared to that of dihybrid-1 catalyst. The trihybrid catalyst can be reused for this functional group transformation reaction (Figure S19). Similarly, in presence of the trihybrid system reduction of 4-nitroaniline to 1,4-phenelenediamine is faster than that of dihybrid-1 gel (Py-W/AuNPs; Figure S20). The mechanism of heterogeneous catalysis reaction depends on several factors, mainly the adsorption behavior and the concentration of the reacting molecule. It is necessary for reactants (aromatic nitro compounds) to come in contact with gold nanoparticles. In this case, the large π-surface of graphene oxide (GO) can promote the adsorption of the reactants through π–π interactions.[8] Such adsorption provides a high effective concentration of 4-nitrophenol near the AuNPs on the GO surface. This facilitates the electron transfer process between metal and GO. All above observations indicate that the presence of the GO support leads to a better catalytic efficiency for the reduction of the aromatic nitro group in 4-nitrophenol and 4-nitroaniline than that in Py-W/AuNPs because of a synergistic effect of the Py-W/GO/AuNPs composite. The modulation of the catalytic property of AuNPs in the presence of carbon-based nanomaterials (GO sheets) in a trihybrid system shines light on the design of noble-metal-based catalysts with a GO support in a hybrid system.

A novel hydrogel-based trihybrid system has been constructed from a pyrene-conjugated single amino acid derivative (Py-W), graphene oxide (GO), and gold nanoparticles (AuNPs). Three distinct morphologies: nanofibers, nanosheet, and nanoparticles, are observed in the corresponding TEM study. At first, Py-W has been found to form a supramolecular hydrogel and this gelator molecule contains planar aromatic pyrene groups and the aromatic, redox-active Trp residue. These aromatic moieties interact with the large π-surface area of graphene oxide (GO) to form a GO-containing hybrid hydrogel. Addition of gold salts (Au^{3+}) within the hybrid hydrogel gives rise to the in situ reduction of Au^{3+} to Au^0, but not to the reduction of GO to reduced GO. Rheological studies reveal that the stiffness of the gel increases with the inclusion of GO into the native gel and the stiffness of this hybrid gel increases further because of the incorporation of gold nanoparticles into the GO-containing hybrid hydrogel in a trihybrid system. Moreover, catalytic property of AuNPs can be tuned from AuNPs containing hybrid gel to trihybrid gel containing Py-W, GO, and gold nanoparticles. Manipulation of the rheological and catalytic behavior will lead to novel, fascinating, and advanced nanomaterials with tunable properties.

Received: February 7, 2013
Published online: April 8, 2013

Keywords: catalysis · hybrid hydrogels · nanoparticles · soft matter

[1] a) A. R. Hirst, B. Escuder, J. F. Miravet, D. K. Smith, *Angew. Chem.* **2008**, *120*, 8122–8139; *Angew. Chem. Int. Ed.* **2008**, *47*, 8002–8018; b) S. S. Babu, S. Prasanthkumar, A. Ajayaghosh, *Angew. Chem.* **2012**, *124*, 1800–1810; *Angew. Chem. Int. Ed.* **2012**, *51*, 1766–1776.

[2] a) A. Wicklein, S. Ghosh, M. Sommer, F. Würthner, M. Thelakkat, *ACS Nano* **2009**, *3*, 1107–1114; b) M. P. Aldred, A. J. Eastwood, S. M. Kelly, P. Vlachos, A. E. A. Contoret, S. R. Farrar, B. Mansoor, M. O'Neill, W. C. Tsoi, *Chem. Mater.* **2004**, *16*, 4928–4936; c) P. Mukhopadhyay, Y. Iwashita, M. Shirakawa,

S.-i. Kawano, N. Fujita, S. Shinkai, *Angew. Chem.* **2006**, *118*, 1622 – 1625; *Angew. Chem. Int. Ed.* **2006**, *45*, 1592 – 1595; d) S. R. Jadhav, P. K. Vemula, R. Kumar, S. R. Raghavan, G. John, *Angew. Chem.* **2010**, *122*, 7861 – 7864; *Angew. Chem. Int. Ed.* **2010**, *49*, 7695 – 7698; e) D. M. Wood, B. W. Greenland, A. L. Acton, F. Rodríguez-Llansola, C. A. Murray, C. J. Cardin, J. F. Miravet, B. Escuder, I. W. Hamley, W. Hayes, *Chem. Eur. J.* **2012**, *18*, 2692 – 2699; f) S. Ray, A. K. Das, A. Banerjee, *Chem. Mater.* **2007**, *19*, 1633 – 1639; g) W. T. Truong, Y. Su, J. T. Meijer, P. Thordarson, F. Braet, *Chem. Asian J.* **2011**, *6*, 30 – 42; h) J. A. Foster, M.-O. M. Piepenbrock, G. O. Lloyd, N. Clarke, J. A. K. Howard, J. W. Steed, *Nat. Chem.* **2010**, *2*, 1037 – 1043.

[3] a) H. Basit, A. Pal, S. Sen, S. Bhattacharya, *Chem. Eur. J.* **2008**, *14*, 6534 – 6545; b) J. van Herrikhuyzen, S. J. George, M. R. J. Vos, N. A. J. M. Sommerdijk, A. Ajayaghosh, S. C. J. Meskers, A. P. H. J. Schenning, *Angew. Chem.* **2007**, *119*, 1857 – 1860; *Angew. Chem. Int. Ed.* **2007**, *46*, 1825 – 1828; c) N. M. Sangeetha, S. Bhat, G. Raffy, C. Belin, A. Loppinet-Serani, C. Aymonier, P. Terech, U. Maitra, J.-P. Desvergne, A. D. Guerzo, *Chem. Mater.* **2009**, *21*, 3424 – 3432; d) P. K. Vemula, U. Aslam, V. A. Mallia, G. John, *Chem. Mater.* **2007**, *19*, 138 – 140; e) G. Palui, J. Nanda, S. Ray, A. Banerjee, *Chem. Eur. J.* **2009**, *15*, 6902 – 6909; f) N. M. Sangeetha, C. Blanck, T. T. T. Nguyen, C. Contal, P. J. Mésini, *ACS Nano* **2012**, *6*, 8498 – 8507; g) M. S. Lamm, N. Sharma, K. Rajagopal, F. L. Beyer, J. P. Schneider, D. J. Pochan, *Adv. Mater.* **2008**, *20*, 447 – 451.

[4] a) B. Adhikari, J. Nanda, A. Banerjee, *Chem. Eur. J.* **2011**, *17*, 11488 – 11496; b) M. Moniruzzaman, A. Sahin, K. I. Winey, *Carbon* **2009**, *47*, 645 – 650; c) S. K. Samanta, K. S. Subrahmanyam, S. Bhattacharya, C. N. R. Rao, *Chem. Eur. J.* **2012**, *18*, 2890 – 2901; d) S. K. Samanta, A. Gomathi, S. Bhattacharya, C. N. R. Rao, *Langmuir* **2010**, *26*, 12230 – 12236; e) S. Srinivasan, S. S. Babu, V. K. Praveen, A. Ajayaghosh, *Angew. Chem.* **2008**, *120*, 5830 – 5833; *Angew. Chem. Int. Ed.* **2008**, *47*, 5746 – 5749; f) Y. Tian, L. Zhang, P. Duan, F. Liu, B. Zhang, C. Liu, M. Liu, *New J. Chem.* **2010**, *34*, 2847 – 2852.

[5] a) C. N. R. Rao, A. K. Sood, K. S. Subrahmanyam, A. Govindaraj, *Angew. Chem.* **2009**, *121*, 7890 – 7916; *Angew. Chem. Int. Ed.* **2009**, *48*, 7752 – 7777; b) M. J. Allen, V. C. Tung, R. B. Kaner, *Chem. Rev.* **2010**, *110*, 132 – 145; c) X. Huang, X. Qi, F. Boey, H. Zhang, *Chem. Soc. Rev.* **2012**, *41*, 666 – 686.

[6] a) P. V. Kamat, *J. Phys. Chem. Lett.* **2011**, *2*, 242 – 251; b) S. Guo, S. Dong, *Chem. Soc. Rev.* **2011**, *40*, 2644 – 2672; c) P. V. Kamat, *J. Phys. Chem. Lett.* **2010**, *1*, 520 – 527; d) D. Du, J. Liu, X. Zhang, X. Cui, Y. Lin, *J. Mater. Chem.* **2011**, *21*, 8032 – 8037; e) Y. Wang, S. Zhang, D. Du, Y. Shao, Z. Li, J. Wang, M. H. Engelhard, J. Li, Y. Lin, *J. Mater. Chem.* **2011**, *21*, 5319 – 5325; f) J. Ma, J. Zhang, Z. Xiong, Y. Yong, X. S. Zhao, *J. Mater. Chem.* **2011**, *21*, 3350 – 3352; g) X. Huang, X. Zhou, S. Wu, Y. Wei, X. Qi, J. Zhang, F. Boey, H. Zhang, *Small* **2010**, *6*, 513 – 516.

[7] a) H. Bai, C. Li, X. Wang, G. Shi, *J. Phys. Chem. C* **2011**, *115*, 5545 – 5551; b) C. Huang, H. Bai, C. Li, G. Shi, *Chem. Commun.* **2011**, *47*, 4962 – 4964; c) Y. Xu, Q. Wu, Y. Sun, H. Bai, G. Shi, *ACS Nano* **2010**, *4*, 7358 – 7362; d) H. Bai, C. Li, X. Wang, G. Shi, *Chem. Commun.* **2010**, *46*, 2376 – 2378; e) S.-Z. Zu, B.-H. Han, *J. Phys. Chem. C* **2009**, *113*, 13651 – 13657; f) B. Adhikari, A. Biswas, A. Banerjee, *Langmuir* **2012**, *28*, 1460 – 1469; g) B. Adhikari, A. Biswas, A. Banerjee, *ACS Appl. Mater. Interfaces* **2012**, *4*, 5472 – 5482.

[8] G. R. Desiraju, A. Gavezzotti, *J. Chem. Soc. Chem. Commun.* **1989**, 621 – 623.

[9] S. Si, T. K. Mandal, *Chem. Eur. J.* **2007**, *13*, 3160 – 3168.

[10] a) M.-O. M. Piepenbrock, N. Clarke, J. W. Steed, *Soft Matter* **2010**, *6*, 3541 – 3547; b) G. Palui, A. Garai, J. Nanda, A. K. Nandi, A. Banerjee, *J. Phys. Chem. B* **2010**, *114*, 1249 – 1256; c) B. Roy, P. Bairi, A. Saha, A. K. Nandi, *Soft Matter* **2011**, *7*, 8067 – 8076; d) S. Bhattacharya, A. Srivastava, A. Pal, *Angew. Chem.* **2006**, *118*, 3000 – 3003; *Angew. Chem. Int. Ed.* **2006**, *45*, 2934 – 2937; e) T. Kar, S. Dutta, P. K. Das, *Soft Matter* **2010**, *6*, 4777 – 4787.

[11] X. Ling, L. Xie, Y. Fang, H. Xu, H. Zhang, J. Kong, M. S. Dresselhaus, J. Zhang, Z. Liu, *Nano Lett.* **2010**, *10*, 553 – 561.

[12] J. Li, C.-y. Liu, Y. Liu, *J. Mater. Chem.* **2012**, *22*, 8426 – 8430.

